

CONSOLFOOD 2018 – International Conference on Advances in Solar Thermal Food Processing  
Faro-Portugal, 22-24 January, 2018

## **SIMULATION OF A SOLAR ASSISTED COUNTERFLOW TUNNEL DEHYDRATOR**

**Carrillo-Andrés, A., Sojo-Gordillo, J.M., Domínguez-Muñoz, F., Cejudo-López, J.M.**

University of Málaga, Industrial Engineering School, Energy Research Group. C/ Arquitecto Peñalosa s/n.  
29071. Spain, Phone: 34-951-952-401, e-mail: [acarrillo@uma.es](mailto:acarrillo@uma.es)

**Abstract:** A widely used class of vegetable dehydration systems are the “tunnel-and-truck” dehydrators, where the prepared material lies over horizontal trays stored in trucks which move discontinuously in opposite direction of the air flow. This way the driest product is facing the inlet hot and dry air blown to the system. When product of one truck is ready, is removed from the tunnel leaving space for advance the remaining truck one place forward. This way, a new truck full of wet product can be inserted at the end of the tunnel. The thermal energy required for the process can be supplied by several sources including gas, biomass, solar energy or a combination of them. Solar energy is for free but reaches the Earth with quite a low flux and a strongly fluctuating rate. This imposes the need of special designs and control strategies. This paper presents a study based on simulation models of the dehydrator and the solar thermal system. The dehydrator simulation model is tuned to match experimental data from a particular prototype based on fossil fuel. A solar system simulation model is then applied to the analysis of different design options.

**Keywords:** Dehydrator, Dryer, Thermal, Solar, Food processing

## 1. INTRODUCTION

A widely used class of vegetable dehydration systems are the “tunnel-and-truck” dehydrators [1]. A schematic can be seen in Figure 1. An electric fan moves air (2-3) through a hot water heating coil (3-4), and then across several trucks loaded with the product to be dehydrated (4-5). The humidity content of the air increases while its temperature decreases, as the air and the product exchange mass and heat. Then some air must be exhausted and replaced with fresh outside air in order to reject some moisture to the environment (6) and keep the drying process going on. A recovery sensible heat exchanger is used to reduce the amount of energy needed to condition the incoming fresh air.

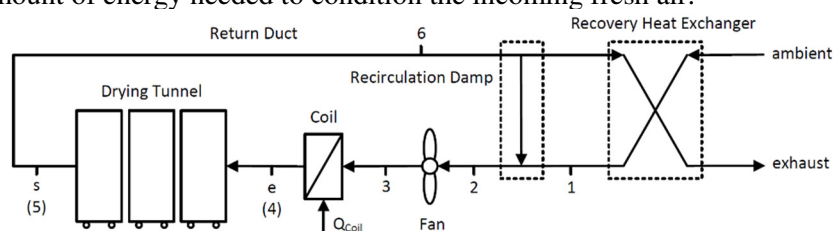


Figure 1. Schematic of the system components.

A prototype of a five-truck dehydrator has been tested experimentally. The prototype has a gas boiler and a hot water heating coil. This paper presents a preliminary evaluation of the potential use of solar energy to reduce the dehydrator fuel consumption. A simulation model of the dehydrator was developed and tuned to match experimental data. Then a simulation model of a solar water heating system is used to analyze different design options.

## 2. EXPERIMENTAL TESTS

Several tests were conducted on the dehydrator prototype but, at the time of writing, only partial load tests (only the first truck loaded) could be completed successfully. A particular test, dehydrating sliced bananas, with a process air temperature set point of 60 °C is taken as the reference test, see Table 1.

Table 1. Parameters and measurements of the reference test. Only the truck #1 is loaded with sliced bananas.

Parameter	Value	Comment
Outside air temperature (°C) and relative humidity (%)	Around 20°C 50 %	Measured
Process air setpoint temperature (°C)	60	Measured
Process air mass flow rate (kg/h)	18906	Measured with digital vane probe
Exhaust air mass flow rate (kg/h)	945	Measured, it is 5% of the process flow rate
Global heat loss coefficient UA (W/C)	110	Determined from stationary heating tests
Heat recovery efficiency	0.8	Calculated from measurements
Fan motor electrical consumption (kW)	2.35	Measured
Wet product initial weight per truck (kg)	81.3	Measured
Dry product weight per truck (kg)	21.1	Estimated
Total water loss (kg)	58	Measured with a weight scale under truck #1
Heating coil energy (kWh)	104	Measured with an energy meter
Fan motor heat energy (kWh)	38	Measured with an energy meter
Heat loss to ambient (kWh)	70	Calculated from UA and temp. differences
Heat loss due to exhaust (kWh)	32	Calculated from energy and mass balances
Dehydration latent energy (kWh)	38	Calculated from product weight loss

The prototype has a weight scale under truck #1 so the weight can be continuously measured and recorded, from the beginning to the end of the test, see Figure 2.

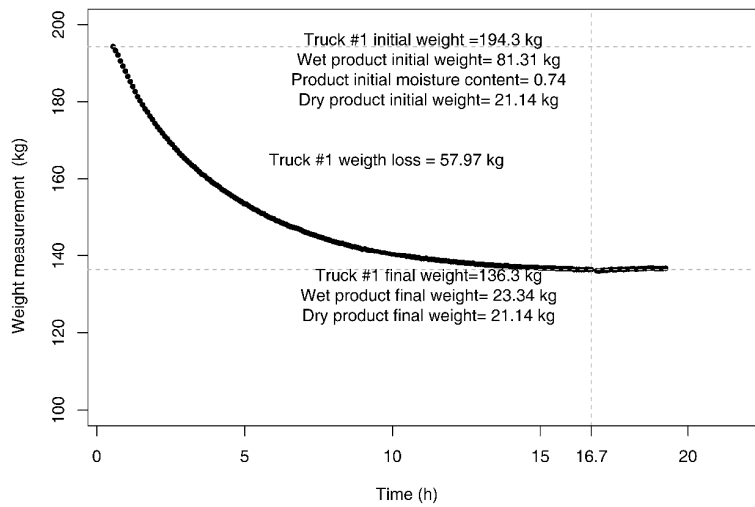


Figure 2. Truck #1 weight versus time for the reference test.

Is interesting to analyze the different thermal energy rate magnitudes in order to check the energy balance, see Figure 3. In spite of some noisy data, there is a good balance between thermal power input ( $Q_{coil} + Q_{fan}$ ) and thermal power output ( $Q_{lat.sc} + Q_{loss} + Q_{ex}$ ).

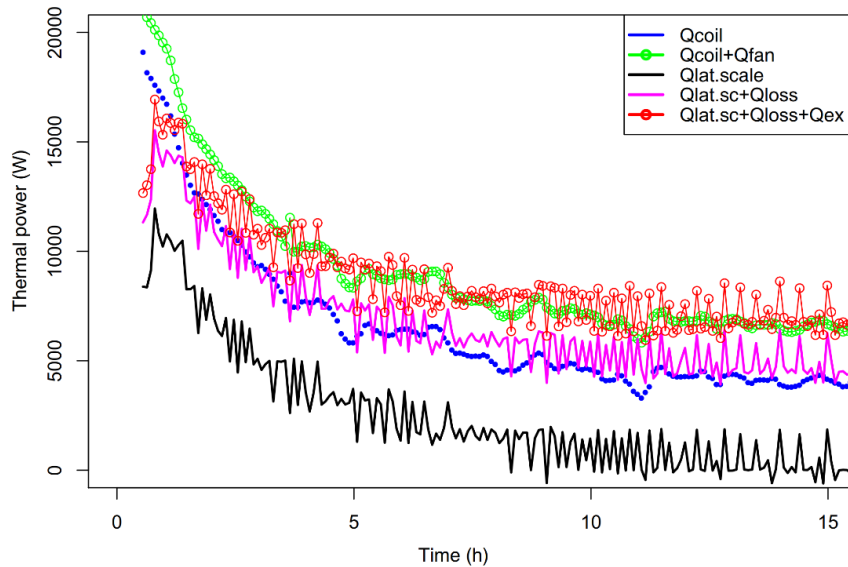


Figure 3. Energy balance. **Qcoil**: Hot water heating coil power, calculated as the first derivative of the hot water energy meter readings. **Qfan**: Electric power absorbed by the fan electric motor. The heat is intended to go into the air stream. **Qlat.scale**: Thermal power associated to the evaporation of water from the product. Calculated from the latent heat of water and the evaporation rate, calculated as the first derivative of the weight scale readings. **Qloss**: Thermal losses to the environment, calculated with the global UA and the temperature difference dehydrator - ambient. **Qex**: Thermal power to condition incoming fresh air.

## 2. DEHYDRATOR MODEL

A model of the dehydrator is programmed using EES[2]. Besides the usual psychrometrics and energy and mass balances involved, there is a key point to be modelled: the drying rate of the product. This rate is clearly variable along the process. From the Figure 2 data, the normalized drying rate of the product in dry basis can be computed and plotted versus the product moisture content excess, see Figure 4. There is a clear dependence between both magnitudes. A third degree polynomial fits well the experimental data. The same procedure is then applied to another reference test with a process air setpoint of 50 °C. A linear interpolation is then applied to find the drying rate for any other temperature in the range 50-60 °C. Obviously this quite simple approach is only valid for this particular dehydrator, product, and operating conditions.

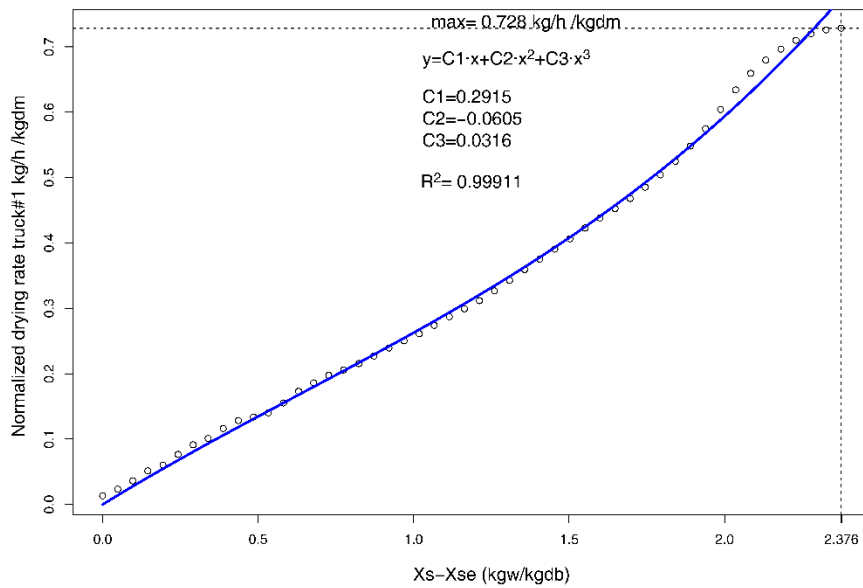


Figure 4. Normalized drying rate vs product dry basis moisture content excess for the reference test with the process air setpoint set at 60 °C

In order to check the model, the reference tests are reproduced with a good agreement between experimental and simulation data, see Figure 5. Then the model is used to simulate a full load operation scenario, that is, the five trucks loaded with product. The other operating conditions remains the same as in the reference test, except the exhaust flow rate, that is increased from 5% to a 25% of the process flow rate. The simulation results (Figure 6) show how the process air temperature drops across the trucks, and how the difference between trucks decreases along time, as was expected. The thermal power required in the heating coil is a very important result, see Figure 7. It starts around 70kW and decreases along time, as the drying rate does. This curve will be the energy demand for the thermal solar system,

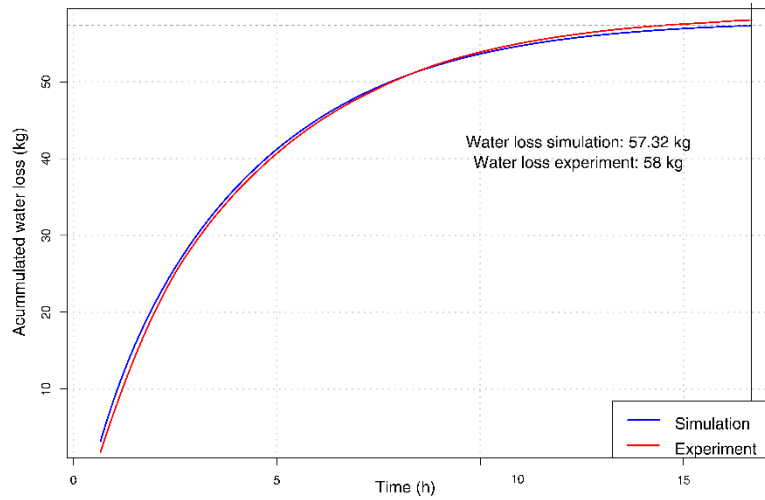


Figure 5. Accumulated water loss. Simulation vs experiment.

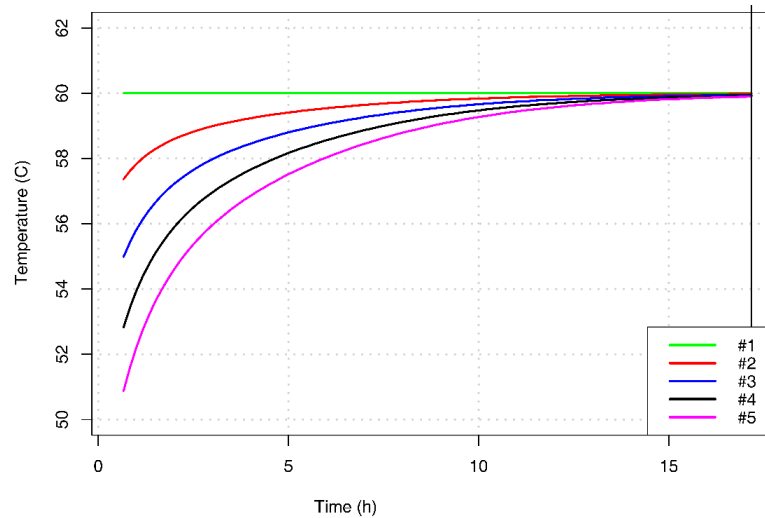


Figure 6. Process air temperature at the inlet of each truck in the full load simulation scenario.

### 3. SOLAR THERMAL SYSTEM MODEL

TRNSYS [3] is used to model a solar thermal system located in Tenerife (Spain), see Table 2. This location is selected because it is an important banana production area. Several simulations are conducted for a range of collector areas and tank volume to collector area ratios. In addition to that, two different strategies for controlling the heating coil are tested. In the first strategy the back-up heater setpoint temperature is set at a constant value of 80 °C. To manage partial load there is a tempering valve to reduce the effective inlet water temperature to the coil by recirculating some flow rate from the coil outlet. In this way the flow rate discharged from the solar tank is reduced. In the second strategy, the back-up heater setpoint temperature is reduced at partial load and the flow rate discharged from the solar tank is always maximum. The process air setpoint temperature is set at a constant value of 60 °C.

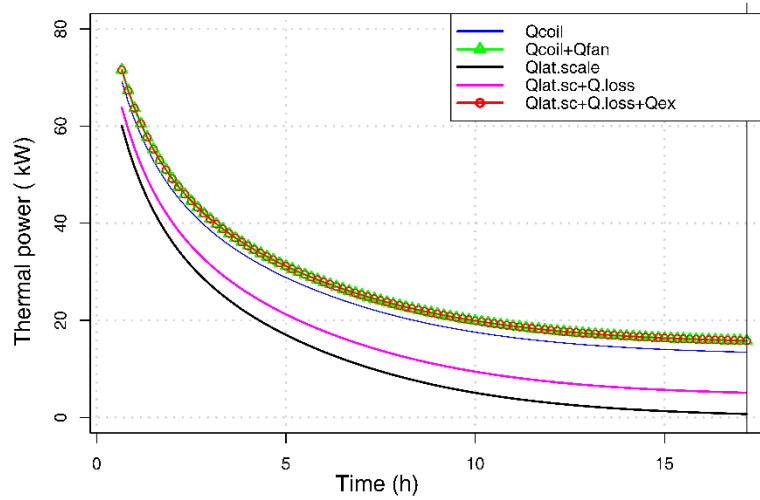


Figure 7. Energy magnitudes in the full load simulation scenario. There is a balance between thermal power input ( $Q_{coil} + Q_{fan}$ ) and thermal power output ( $Q_{lat.sc} + Q_{loss} + Q_{ex}$ )

Table 2. Parameters of the solar thermal system.

Parameter	Value	Comment
Weather file	Tenerife.EPW	EnergyPlus weather data [4]. Lat: 28.47 °N
Energy demand from drehydrator (kW)	$Q_{coil}$ from Fig 7	A batch operation is assumed starting at 16h every day of the year and finishing at 9h next day.
Collector type	select. flat plate	$C_0=0.809$ $C_1=4.030$ $W/m^2K$ $C_2=0.007$ $W/m^2K^2$
Slope and azimuth	30 ° facing south	Typical parameters
Collector area ( $m^2$ )	50 to 300	Aperture area
Solar tank volume to col. area ratio VA ( $l/m^2$ )	50-75-100	Typical range
Collectors arrangement	2 units in series	Typical arrangement
Solar field flow rate ratio ( $l/hm^2$ )	40	Nominal value for the selected collector.
Thermal losses in piping	Neglected	This is a preliminary analysis
Solar tank insulation	100 mm	$k=0.04$ $W/mK$
Maximum temperature allowed in tank (°C)	90	Typical value
Back-up heater position	Series with tank	An “ideal” back-up heater is assumed
Back-up heater setpoint temperature (°C)	80 or variable	Two different control strategies, see text
Heating coil nominal thermal power (kW)	70	Data from the simulation of the full load test Fig7
Heating coil air flow rate (kg/h)	18906	Actual air flow rate in the prototype
Heating coil water flow rate (kg/h)	4225	A balanced heat exchanger is assumed
Heating coil nominal air temperatures (°C)	47 inlet 60 outlet	60 °C is the process air setpoint, 47 °C from simulation of the full load scenario Fig.7.
Heating coil nominal water temp. (°C)	80 inlet 67 outlet	80 °C is the water temperature setpoint of the boiler of the prototype.
Heating coil exchange effectiveness	0.4	Calculated from assumptions above

#### 4. RESULTS AND CONCLUSIONS

Two figures of merit are used to measure the performance of the solar system: a) the solar fraction (SF), defined as the fraction of the total load which is covered by solar energy, and b) the net collector

efficiency (NCE), defined as the fraction of useful solar heat with respect to the solar radiation incident on the collector. The Figure 8 shows a huge improvement in performance when the VA ratio increases from 50 to 75 l/m<sup>2</sup> (but not so much from 75 to 100). The variable setpoint temperature control strategy also improves the performance of the solar system, and it is very dependent on the VA ratio and the collector area. The improvement is negligible for cases with low SF, and maximum when SF is around 75-80 %. For example, for the case with VA=75 l/m<sup>2</sup> and A=175 m<sup>2</sup>, the SF increases from 76.8% to 82.3% (5.5 points). The NCE is around 35% for cases with VA 75-100 l/m<sup>2</sup>, collector area up to 150 m<sup>2</sup> and variable back-up setpoint control, and then shows a marked decline for larger areas. This paper presents a preliminary analysis: there still remains several aspects to be researched in how the dehydrator and solar system perform together under different operating conditions.

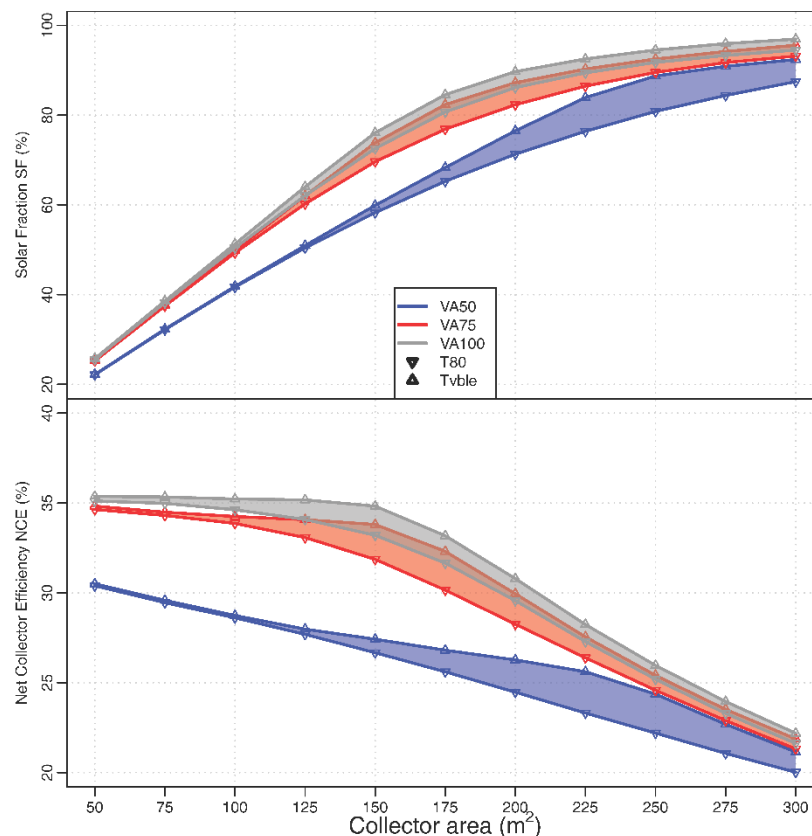


Figure 8. Solar Fraction and Net Collector Efficiency for the solar system.

## REFERENCES

- [1] W.. Van Arsdel, Tunnel-and-truck dehydrators, as used for dehydrating vegetables, en: Veg. fruit dehydration, a Man. plant Oper., 1944. doi:10.1007/s13398-014-0173-7.2.
- [2] S.A. Klein, EES (Engineering Equation Solver), (s. f.). www.fchart.com.
- [3] S.A. Klein, J.A. Duffie, W.A. Beckman, TRNSYS 16: A transient system simulation program., (2007). <https://sel.me.wisc.edu/>.
- [4] D.O.E., EnergyPlus, (2015). www.energyplus.net.